

Linear Free Energy Relationships for Complex Formation Reactions between Carboxylic Acids and Palladium(II). Equilibrium and High-Pressure Kinetics Study

Tiesheng Shi and Lars I. Elding*

Inorganic Chemistry 1, Chemical Center, Lund University, P. O. Box 124, S-221 00 Lund, Sweden

Received November 8, 1996[⊗]

Kinetics for complex formation between $\text{Pd}(\text{H}_2\text{O})_4^{2+}$ and formic, butyric, DL-lactic, 2-methylactic, methoxyacetic, malonic, succinic, oxydiacetic, L-malic, and citric acids has been studied in an aqueous acidic medium by use of variable-temperature and -pressure stopped-flow spectrophotometry. Kinetics traces for reactions between the metal ion and formic, butyric, lactic, 2-methylactic, methoxyacetic, oxydiacetic, and citric acids can be described by single exponentials, which are assigned to the formation of monodentate complexes: $\text{Pd}(\text{H}_2\text{O})_4^{2+} + \text{RCOOH} \rightleftharpoons \text{Pd}(\text{H}_2\text{O})_3\text{OOCR}^+ + \text{H}_3\text{O}^+$ (k_1 , k_{-1}). Equilibrium constants K_1 for lactic, 2-methylactic, methoxyacetic, oxydiacetic, and citric acid reactions calculated from spectrophotometric equilibrium measurements and from kinetics ($K_1 = k_1/k_{-1}$) are in good agreement. There is a linear correlation between the stability constants β_1 of the carboxylato complexes and the first dissociation constants K_{a1} of the carboxylic acids as expressed by $\log \beta_1 = (0.48 \pm 0.03)\text{p}K_{a1} + (2.1 \pm 0.1)$. The formation rate constants k_1 are insensitive to the basicity and steric properties of the carboxylic acids at 25 °C, due to an excellent isokinetic relationship between ΔH_1^\ddagger and ΔS_1^\ddagger with an isokinetic temperature of 292 K, suggesting also that all of the carboxylic acids react via the same mechanism. Rate constants k_{-1} are correlated with $\text{p}K_{a1}$ of the entering carboxylic acids according to $\log k_{-1} = (0.47 \pm 0.06)\text{p}K_{a1} - (0.7 \pm 0.2)$, indicating that the weaker the carboxylic acid, the larger k_{-1} . These facts together with the observation that a weak carboxylic acid is prone to form a strong complex as shown by the correlation between $\log \beta_1$ and $\text{p}K_{a1}$ are interpreted in terms of a proton-assisted reaction mechanism which is further supported by the ionic strength dependence of the rate constant k_{-1} , consistent with a direct attack of an oxonium ion on $\text{Pd}(\text{H}_2\text{O})_3\text{OOCR}^+$ for the reverse reaction. High-pressure stopped-flow measurements at 25 °C give activation volumes $\Delta V_1^\ddagger = -4.9 \pm 0.2 \text{ cm}^3 \text{ mol}^{-1}$, $\Delta V_{-1}^\ddagger = -2.7 \pm 0.5 \text{ cm}^3 \text{ mol}^{-1}$ for malonic acid, and $\Delta V_1^\ddagger = -3.5 \pm 0.2 \text{ cm}^3 \text{ mol}^{-1}$, $\Delta V_{-1}^\ddagger = -1.9 \pm 0.4 \text{ cm}^3 \text{ mol}^{-1}$ for citric acid, respectively. Existing data so far for $\text{Pd}(\text{H}_2\text{O})_4^{2+}$ complex formation reactions obey a linear correlation between ΔV_1^\ddagger and partial molar reaction volumes ΔV_1° according to $\Delta V_1^\ddagger = (0.92 \pm 0.04)\Delta V_1^\circ - (2.2 \pm 0.2) \text{ cm}^3 \text{ mol}^{-1}$, the slope of 0.92 indicating that bond-making between palladium and the entering ligands largely dominates the formation of the transition state. There are no linear correlations between ΔV_1^\ddagger and partial molar volumes V_L of the entering ligands, as has been claimed in previous literature for related reactions, or between ΔV_1^\ddagger and ΔS_1^\ddagger .

Introduction

Linear free energy relationships are useful in diagnosis of reaction mechanisms. In coordination chemistry, such relationships have been extensively used for reactions of octahedral complexes.¹ Applications to square-planar reactions are much less common due to limited experimental information. A main object of the present study has been to apply various types of linear free energy relationships to square-planar substitution processes, using rate and equilibrium data for a large series of related reactions, including also variable-temperature and -pressure data.

The reactivity of polyatomic ligands with a constant donor atom and varying substituents toward metal centers can often be expressed in terms of steric and electronic contributions. For square-planar complexes, studies of how variation of donor atom substituents affects the reactivity have been performed for N-, P-, and S-donor ligands.^{2–9} Such studies can give quantitative information on the relative importance of steric and electronic contributions in the activation process and on the molecular mechanism of the complex formation reaction. The present

work is an extension of previous structure–reactivity studies of thioethers as nucleophiles in square-planar substitution reactions⁹ to polyatomic oxygen-bonded ligands, viz., a series of carboxylic acids with largely varying basicities and steric properties. Together with a previous report,¹⁰ it seems to represent the first systematic investigation of thermodynamics

[⊗] Abstract published in *Advance ACS Abstracts*, January 15, 1997.
 (1) Wilkins, R. G. *Kinetics and Mechanism of Reactions of Transition Metal Complexes*, 2nd ed.; VCH: Weinheim, Germany, 1991; pp 93–110.
 (2) (a) Cattalini, L.; Orio, A. *J. Am. Chem. Soc.* **1968**, *90*, 4800–4803.
 (b) Cattalini, L.; Martelli, M. *J. Am. Chem. Soc.* **1969**, *91*, 312–316.

(3) (a) Cattalini, L.; Marangoni, G.; Michelon, G.; Paolucci, G.; Tobe, M. L. *Inorg. Chem.* **1981**, *20*, 71–75. (b) Bonivento, M.; Canovese, L.; Cattalini, L.; Marangoni, G.; Michelon, G.; Tobe, M. L. *Inorg. Chem.* **1981**, *20*, 1493–1496. (c) Gosling, R.; Tobe, M. L. *Inorg. Chem.* **1983**, *22*, 1235–1244. (d) Cattalini, L.; Chessa, G.; Michelon, G.; Pitteri, B.; Tobe, M. L.; Zanardo, A. *Inorg. Chem.* **1985**, *24*, 3409–3413. (e) Bellicini, M.; Cattalini, L.; Marangoni, G.; Pitteri, B. *J. Chem. Soc., Dalton Trans.* **1994**, 1805–1811. (f) Pitteri, B.; Marangoni, G.; Cattalini, L. *J. Chem. Soc., Dalton Trans.* **1994**, 3539–3543.
 (4) Romeo, R.; Arena, G.; Scolaro, L. M.; Plutino, M. R.; Bruno, G.; Nicolo, F. *Inorg. Chem.* **1994**, *33*, 4029–4037.
 (5) Romeo, R.; Arena, G.; Scolaro, L. M. *Inorg. Chem.* **1992**, *31*, 4879–4884.
 (6) (a) Cattalini, L.; Marangoni, G.; Martelli, M. *Inorg. Chem.* **1968**, *7*, 1495–1499. (b) Cattalini, L.; Martelli, M.; Kirscher, G. *Inorg. Chem.* **1968**, *7*, 1488–1492. (c) Bonivento, M.; Canovese, L.; Cattalini, L.; Marangoni, G.; Michelon, G.; Tobe, M. L. *Inorg. Chem.* **1983**, *22*, 802–805.
 (7) Jones, T. E.; Cole, J. R.; Nusser, B. J. *Inorg. Chem.* **1978**, *17*, 3680–3684.
 (8) Annibale, G.; Cattalini, L.; Canovese, L.; Michelon, G.; Marangoni, G.; Tobe, M. L. *Inorg. Chem.* **1983**, *22*, 975–978.
 (9) Shi, T.; Elding, L. I. *Inorg. Chem.* **1996**, *35*, 5941–5947.
 (10) Shi, T.; Elding, L. I. *Inorg. Chem.* **1996**, *35*, 735–740.

Table 1. Dissociation Constants and Partial Molar Volumes of Carboxylic Acids at 25 °C and $\mu = 1.0$ M

no.	carboxylic acid	pK_{a1}	pK_{a2}	$V_L / (\text{cm}^3 \text{mol}^{-1})$
1	formic	HCOOH	3.53 ^a	
2	acetic	CH ₃ COOH	4.57 ^a	52, ^e 51.9 ^f
3	propionic	CH ₃ CH ₂ COOH	4.67 ^a	67.9 ^f
4	butyric	CH ₃ CH ₂ CH ₂ COOH	4.68 ^b	84.6 ^f
5	glycolic	HOCH ₂ COOH	3.62 ^a	51.75 ^{g,i}
6	DL-lactic	CH ₃ CH(OH)COOH	3.64 ^a	
7	2-methylactic	(CH ₃) ₂ C(OH)COOH	3.77 ^a	
8	methoxyacetic	CH ₃ OCH ₂ COOH	3.40 ^c	
9	malonic	HOOCCH ₂ COOH	2.60 ^a	5.07 ^a 67.2 ^{h,i}
10	succinic	HOOCCH ₂ CH ₂ COOH	3.95 ^a	5.12 ^a
11	oxydiacetic	HOOCCH ₂ OCH ₂ COOH	2.82 ^d	3.77 ^d
12	L-malic	HOOCCH(OH)CH ₂ COOH	3.11 ^a	4.45 ^a
13	citric	HOOC(OH)(CH ₂ COOH) ₂	2.80 ^a	4.08 ^a 112 ^e

^a Martell, A. E.; Smith, R. M. *Critical Stability Constants, Other Organic Ligands*; Plenum: New York, 1977; Vol. 3, pp 1–161.
^b Brown, K. L.; Zahonyi-Budo, E. *Inorg. Chem.* **1981**, *20*, 1264. ^c Sayer, J. M.; Jencks, W. P. *J. Am. Chem. Soc.* **1969**, *91*, 6353. ^d Grant, P. M.; Robouch, P.; Torres, R. A.; Baisden, P. A.; Silva, R. J. *J. Solution Chem.* **1992**, *21*, 213. ^e Manzurola, E.; Apelblat, A. *J. Chem. Thermodyn.* **1985**, *17*, 579. ^f Høiland, H. *Acta Chem. Scand. A* **1974**, *28*, 699.
^g Høiland, H. *J. Chem. Soc., Faraday Trans. 1* **1975**, *71*, 2007.
^h Høiland, H. *J. Chem. Soc., Faraday Trans. 1* **1975**, *71*, 797. ⁱ $\mu \approx 0.50$ M.

and kinetics for reactions between square-planar complexes and oxygen-bonded ligands.

Experimental Section

Chemicals and Solutions. Stock solutions of tetraaquapalladium(II) perchlorate (ca. 50 mM) in 1.00 or 2.00 M perchloric acid were prepared from palladium sponge (Johnson and Matthey, Spec. pure) and analyzed as described previously.¹¹ Stock solutions of 1.000, 2.000, and 4.00 M perchloric acid were prepared from concentrated acid (Merck, p.a.), and stock solutions of 1.000 M sodium perchlorate was prepared from NaClO₄·H₂O (Merck, p.a.). Formic, butyric, DL-lactic, 2-methylactic, L-malic, methoxyacetic, and citric acids (all Janssen, p.a.), oxydiacetic (Merck, p.a.), and malonic acids (Fluka, 99%) were used directly without further purification. Succinic acid (Aldrich, 98%) was recrystallized from hot water and dried at 120 °C. Dissociation constants of the carboxylic acids for the conditions relevant to the present study are summarized in Table 1, together with their partial molar volumes, V_L . The ionic strength was adjusted with perchloric acid and sodium perchlorate. Water was doubly distilled from quartz.

Apparatus. UV–visible spectra were recorded on a Milton Roy 3000 diode-array spectrophotometer. The kinetics was followed at ambient pressure by use of a modified Durrum-Gibson stopped-flow spectrophotometer or an Applied Photophysics Bio Sequential SX-17 MX stopped-flow ASVD spectrofluorimeter and, at elevated pressures, by use of a Hi-Tech high-pressure stopped-flow spectrophotometer, HPSF-56, equipped with a digital pressure indicator.¹² Temperature was controlled to ± 0.1 °C. Pseudo-first-order rate constants were evaluated using the OLIS nonlinear least-squares-minimizing kinetics program Model 4000 Data System Stopped-Flow Version 9.04¹³ or the Applied Photophysics software package.¹⁴

General Observations. Reactions between Pd(H₂O)₄²⁺ and butyric, lactic, 2-methylactic, methoxyacetic, oxydiacetic, and citric acids could be described by single exponentials. No subsequent reactions were observed. UV-vis spectral changes indicated that complex formation was complete within the time of mixing, and spectra were constant for at least 24 h. In the case of formic acid, a slow reduction of

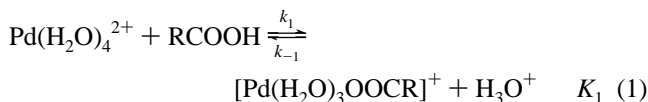
palladium(II) was observed ca. 20 min after the rapid complex formation reaction. For L-malic acid, slow spectral changes were observed after the rapid complex formation reaction, and a black palladium precipitate appeared after ca. 20 h. The reactions with malonic and succinic acids also resulted in slow spectral changes after the rapid substitution process, but no precipitate was observed, and the fast substitution reactions were well-separated in time from these slow processes. The slow reactions occurring after complex formation in the cases of formic, malic, malonic, and succinic acids were not studied further. All equilibrium and kinetics measurements were performed in media with $0.60 \leq [\text{H}^+] \leq 1.00$ M, where hydrolysis of Pd(H₂O)₄²⁺ is negligible (pK_h is ca. 3.0).¹⁵

Measurements. Spectra between 250 and 500 nm of equilibrated solutions with a constant total concentration of palladium and with various pH and concentrations of carboxylic acid (lactic, 2-methylactic, methoxyacetic, oxydiacetic, and citric acids) were recorded at 25 °C. Reactions between Pd(H₂O)₄²⁺ and the carboxylic acids at ambient pressure were initiated by mixing equal volumes of metal and ligand solutions directly in the stopped-flow instruments. They were followed under pseudo-first-order conditions with carboxylic acid in at least 10-fold excess. The observed pseudo-first-order rate constants, k_{obsd} , are given as average values from at least seven independent runs. Complex formation with formic acid is complete within 2 s, so the subsequent slow reduction to metallic palladium has no influence on the rate measurements. For malic, malonic, and succinic acids, the fast kinetics processes can also be fitted to single exponentials since they are well-separated in time from the subsequent much slower reactions. Experimental data are summarized in Supporting Information Tables S1–S10.

The pressure dependencies of the observed rate constants were studied between 0.1 and 150 MPa in the cases of malonic and citric acids. These reactions were also followed under pseudo-first-order conditions with carboxylic acid in excess, $4.9 \leq C_{\text{Pd}} \leq 9.0$ mM, and $[\text{H}^+] = 1.00$ M. High-pressure kinetics data are listed in Supporting Information Tables S11 and S12.

Results

Equilibrium Studies: Monocarboxylic Acids. The kinetics traces follow single exponentials, suggesting that only 1:1 complexes are formed. With formic, butyric, lactic, 2-methylactic, and methoxyacetic acids, monodentate 1:1 complexes are expected to be formed according to eq 1, similar to what



was observed previously for acetic, propionic, and glycolic acids.¹⁰ The observed absorbances of equilibrated solutions, A_{obsd} , as functions of the total concentration of palladium, $[\text{Pd(II)}]_{\text{tot}}$, and that of carboxylic acid, $[\text{RCOOH}]$, can be derived as eq 2 by using $[\text{H}^+] \gg K_{a1}$; A_0 denotes the absorbance at

$$A_{\text{obsd}} = \frac{A_0 + \epsilon_1 l [\text{Pd(II)}]_{\text{tot}} K_1 \{[\text{RCOOH}]/[\text{H}^+]\}}{1 + K_1 \{[\text{RCOOH}]/[\text{H}^+]\}} \quad (2)$$

$[\text{RCOOH}] = 0$, l the path length, and ϵ_1 the molar absorptivity of the complexes formed according to eq 1 with equilibrium constant K_1 . Fits of eq 2 to the experimental data for the reactions of lactic, 2-methylactic, and methoxyacetic acids are given in Supporting Information Figure S1, and the calculated values of K_1 and ϵ_1 are listed in Supporting Information Table S13. The K_1 values derived at different wavelengths are in good agreement. Calculated spectra of the complexes formed are shown in Figure 1, and equilibrium constants K_1 are given in Table 2.

(15) Shi, T.; Elding, L. I. Unpublished results.

(11) Elding, L. I. *Inorg. Chim. Acta* **1972**, *6*, 647–651.

(12) A development of the high-pressure bomb described by: Nichols, P. J.; Ducommun, Y.; Merbach, A. E. *Inorg. Chem.* **1983**, *22*, 3993–3995.

(13) *OLIS kinetic fitting program*; OLIS Inc.: Jefferson, GA, 1988.

(14) *Applied Photophysics Bio Sequential SX-17 MV, Stopped-Flow ASVD Spectrofluorimeter*, software manual; Applied Photophysics Ltd.: Leatherhead, U.K., 1993.

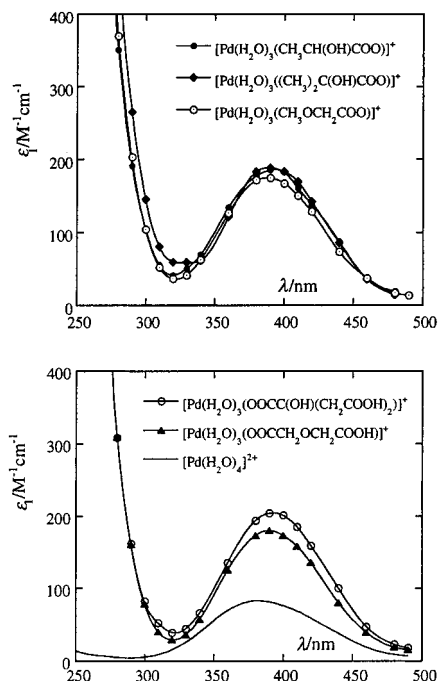


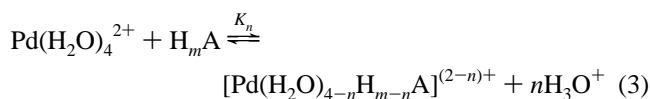
Figure 1. Calculated absorption spectra of monodentate lactate (●), 2-methylactate (◆), methoxyacetate (⊙), dihydrogen citrate (○), and hydrogenoxydiacetate (▲) palladium(II) complexes together with the spectrum of $\text{Pd}(\text{H}_2\text{O})_4^{2+}$.

Table 2. Equilibrium Constants of Reaction 1 Derived from Equilibrium Measurements and from Kinetics for Reactions between $\text{Pd}(\text{H}_2\text{O})_4^{2+}$ and Carboxylic Acids at 25 °C

no.	carboxylic acid	K_1^a	$K_1 = k_1/k_{-1}$
6	DL-lactic	1.2 ± 0.2	1.42 ± 0.03
7	2-methylactate	1.6 ± 0.2	1.88 ± 0.06
8	methoxyacetate	1.7 ± 0.2	1.60 ± 0.05
11	oxydiacetic	4.0 ± 0.6	4.4 ± 0.3
13	citric	4.5 ± 0.6	4.6 ± 0.2

^a Average values derived between 260 and 460 nm; complete data summarized in the Supporting Information Table S13.

Equilibrium Studies: Polycarboxylic Acids. Polycarboxylic acids (H_mA) display various binding modes with metal centers.^{16–21} In the present systems, the number of protons n displaced by palladium (cf. eq 3) can be determined from the



$[\text{H}^+]$ dependence of A_{obsd} . Expressions of A_{obsd} as a function of $[\text{H}_m\text{A}]/[\text{H}^+]^n$ were analyzed for $n = 1$ and 2 in the case of oxydiacetic acid ($m = 2$). For $n = 1$, a plot of A_{obsd} vs $[\text{H}_2\text{A}]/[\text{H}^+]$ is shown in Figure 2. Data analysis according to eq 2 gave a good fit, and values of K_1 and ϵ_1 obtained at various wavelengths are listed in Supporting Information Table S13. A plot of A_{obsd} vs $[\text{H}_2\text{A}]/[\text{H}^+]^2$ for $n = 2$ did not give smooth curves, indicating that this possibility can be eliminated. A similar data analysis for the reaction of citric acid suggests that only one proton is released (Figure S1 and Table S13 in Supporting Information). The calculated spectra of the com-

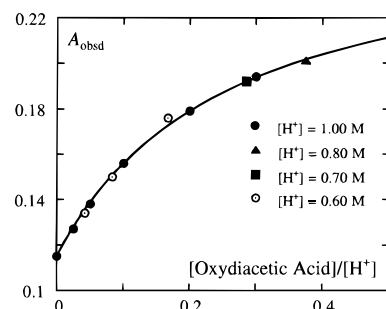


Figure 2. Observed absorbances of equilibrated solutions as a function of $[\text{RCOOH}]/[\text{H}^+]$ for reaction between $\text{Pd}(\text{H}_2\text{O})_4^{2+}$ and oxydiacetic acid at 25 °C and 400 nm. The solid curve represents a nonlinear least-squares fit of eq 2 to the experimental data.

plexes formed with the polycarboxylic acids are very similar to those of the monocarboxylate complexes; cf. Figure 1. These observations, together with the linear free energy relationships derived below, support the conclusion that all of the carboxylic acids studied form 1:1 monodentate complexes with palladium under the experimental conditions used. Equilibrium constants K_1 are listed in Table 2.

Kinetics. It is expected that the mechanism proposed earlier¹⁰ for reaction between $\text{Pd}(\text{H}_2\text{O})_4^{2+}$ and acetic, propionic, and glycolic acids is valid for the present systems too, since only monocarboxylate 1:1 complexes are formed in all cases. By use of Scheme 1 of ref 10 and notations defined therein, eqs 4–6 can be derived as the general expression for the observed

$$k_{\text{obsd}} = k_f[\text{RCOOH}] + k_r \quad (4)$$

$$k_f = k_1 + (k_2K_{a1} + k_3K_h)/[\text{H}^+] + k_4K_{a1}K_h/[\text{H}^+]^2 \quad (5)$$

$$k_r = k_{-1}[\text{H}^+] + k_{-2} + k_{-3} + k_{-4}K_h'/[\text{H}^+] \quad (6)$$

pseudo-first-order rate constants as a function of the total concentration of carboxylic acid, $[\text{RCOOH}]$, and of $[\text{H}^+]$ by use of K_{a1} , K_h , and $K_h' \ll [\text{H}^+]$. Rate constants for the forward and back reactions of the overall process are denoted k_f and k_r , respectively. Kinetics measurements were performed in the range $0.60 \leq [\text{H}^+] \leq 1.00$ M. Linear plots of k_{obsd} vs $[\text{RCOOH}]$ are strictly parallel in this acidity range (cf. Supporting Information Figure S2), indicating that the terms containing k_2 , k_3 , and k_4 in eq 5 are negligible. Moreover, the ratios of $k_f/[\text{H}^+]$ are constant in this acidity range. Thus, the terms containing k_{-2} , k_{-3} , and k_{-4} in eq 6 do not contribute to the overall kinetics and can also be neglected. As a result, Scheme 1 of ref 10 can be reduced conditionally to eq 1. Equations 4–6 can accordingly be simplified to eq 7, which can be further

$$k_{\text{obsd}} = k_1[\text{RCOOH}] + k_{-1}[\text{H}^+] \quad (7)$$

$$k_{\text{obsd}}/[\text{H}^+] = k_{-1} + k_1[\text{RCOOH}]/[\text{H}^+] \quad (8)$$

rearranged as eq 8. Plots according to eq 8 are shown in Figure 3 for monocarboxylic acids and in Figure 4 for polycarboxylic acids. Values of k_1 and k_{-1} calculated by a least-squares fit of eq 8 to the data are listed in Table 3. Activation parameters calculated by use of Eyring's equation from the temperature dependencies of k_1 and k_{-1} are also summarized in Table 3. Equilibrium constants derived from the kinetics as $K_1 = k_1/k_{-1}$ are given in Table 4.

Ionic Strength Dependence. The ionic strength dependence of the rate constants was studied in the case of malic acid. Data are given in Table 5. Within the experimental errors, values

- (16) Mentasti, E. *Inorg. Chem.* **1979**, *18*, 1512–1515.
 (17) Mentasti, E.; Baiocchi, C. *J. Coord. Chem.* **1980**, *10*, 229–237.
 (18) Warner, R. C.; Weber, I. *J. Am. Chem. Soc.* **1953**, *75*, 5086–5094.
 (19) Bobtelsky, M.; Jordan, J. *J. Am. Chem. Soc.* **1945**, *67*, 1824–1831.
 (20) Rajan, K. S.; Martell, A. E. *J. Inorg. Nucl. Chem.* **1964**, *26*, 1927–1944; *Inorg. Chem.* **1965**, *4*, 462–469.
 (21) Hanna, S. B.; Sarac, S. A. *J. Org. Chem.* **1977**, *42*, 2069–2073.

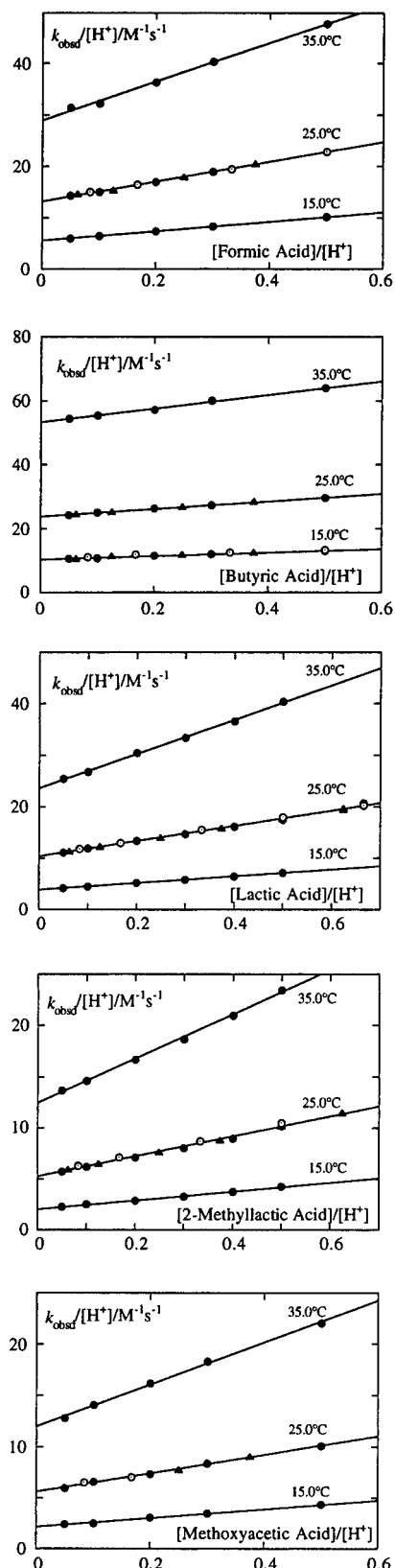


Figure 3. $k_{\text{obsd}}/[\text{H}^+]$ as a function of $[\text{RCOOH}]/[\text{H}^+]$ according to eq 8 for monocarboxylic acids. Hydrogen ion concentrations are 0.60 (\odot), 0.80 (\blacktriangle), and 1.00 M (\bullet).

of k_1 are independent of ionic strength which is consistent with a reaction with a noncharged carboxylic acid molecule, eq 1. On the other hand, values of k_{-1} increase from 4.8 to 6.8 $\text{M}^{-1} \text{s}^{-1}$ when the ionic strength is increased from 0.50 to 2.00 M, which is in quantitative agreement with a reaction between two similarly charged species. In spite of the very high ionic

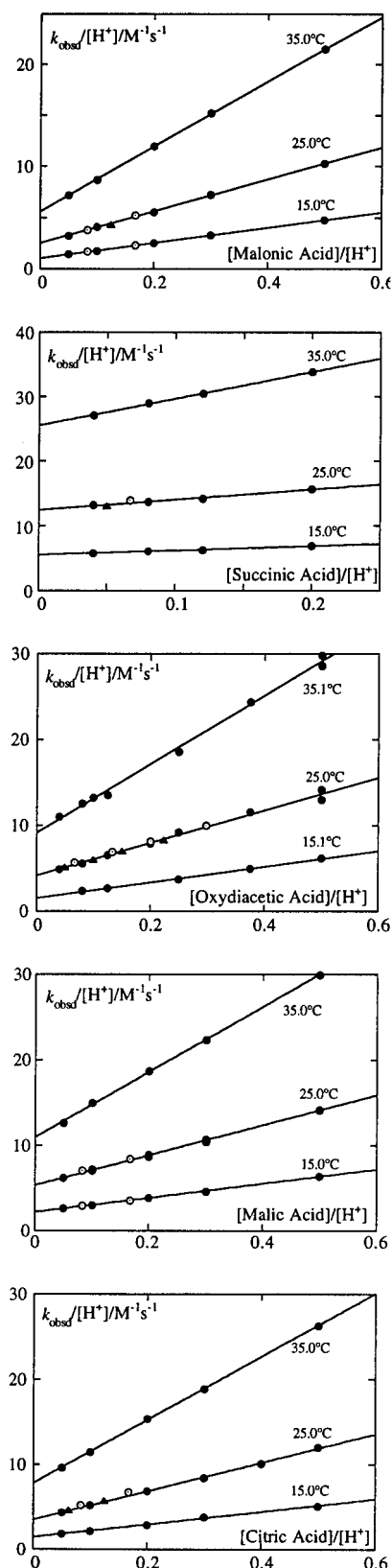


Figure 4. $k_{\text{obsd}}/[\text{H}^+]$ as a function of $[\text{RCOOH}]/[\text{H}^+]$ according to eq 8 for polycarboxylic acids. Hydrogen ion concentrations are 0.60 (\odot), 0.80 (\blacktriangle), and 1.00 M (\bullet).

strength used, a rough linear plot of $\log k_{-1}$ vs $\mu^{1/2}/(1 + \mu^{1/2})$ according to the usual equation for the ionic strength dependence of rate constants,²² using the data in Table 5, yields $Z_A Z_B = +0.8 \pm 0.2$.

Table 3. Rate Constants k_1 and k_{-1} and Activation Parameters (ΔH_1^\ddagger , ΔS_1^\ddagger , ΔV_1^\ddagger , ΔH_{-1}^\ddagger , ΔS_{-1}^\ddagger , and ΔV_{-1}^\ddagger) for Reactions of $\text{Pd}(\text{H}_2\text{O})_4^{2+}$ with Carboxylic Acids at $\mu = 1.00$ M

no.	carboxylic acid	$k_1^{298}/$ ($\text{M}^{-1} \text{s}^{-1}$)	$k_{-1}^{298}/$ ($\text{M}^{-1} \text{s}^{-1}$)	$\Delta H_1^\ddagger/$ (kJ mol^{-1})	$\Delta S_1^\ddagger b/$ ($\text{J K}^{-1} \text{mol}^{-1}$)	$\Delta V_1^\ddagger b/$ ($\text{cm}^3 \text{mol}^{-1}$)	$\Delta H_{-1}^\ddagger/$ (kJ mol^{-1})	$\Delta S_{-1}^\ddagger b/$ ($\text{J K}^{-1} \text{mol}^{-1}$)	$\Delta V_{-1}^\ddagger b/$ ($\text{cm}^3 \text{mol}^{-1}$)
1	formic	19.0 ± 0.1	13.3 ± 0.1	49.2 ± 0.4	-55 ± 1		58.9 ± 1.0	-26 ± 3	
2	acetic ^a	19.3 ± 0.6	32.8 ± 0.2	52.5 ± 0.4	-44 ± 1	-8.1 ± 0.3	57.5 ± 0.4	-23 ± 1	-1.7 ± 0.2
3	propionic ^a	12.0 ± 1.1	26.4 ± 0.3	55.3 ± 0.6	-32 ± 2	-8.9 ± 0.8	56.8 ± 0.3	-34 ± 1	-1.7 ± 0.2
4	butyric	12.1 ± 0.3	23.8 ± 0.1	43.5 ± 1.8	-78 ± 6		58.1 ± 0.8	-24 ± 3	
5	glycolic ^a	21.1 ± 0.3	13.7 ± 0.1	53.6 ± 0.4	-40 ± 1	-3.4 ± 0.2	59.2 ± 0.6	-25 ± 2	-2.3 ± 0.2
6	DL-lactic	14.8 ± 0.2	10.4 ± 0.1	57.2 ± 1.2	-30 ± 4		63.8 ± 2.1	-12 ± 7	
7	2-methylactic	9.9 ± 0.2	5.5 ± 0.1	56.4 ± 0.5	-36 ± 2		64.5 ± 0.8	-15 ± 3	
8	methoxyacetic	9.0 ± 0.2	5.6 ± 0.1	54.2 ± 3.4	-44 ± 11		61.0 ± 3.0	-26 ± 10	
9	malonic	15.7 ± 0.2	2.5 ± 0.1	51.4 ± 0.1	-49 ± 1	-4.9 ± 0.2	58.9 ± 0.2	-39 ± 1	-2.7 ± 0.5
10	succinic	15.4 ± 2.0	12.6 ± 0.2	64.1 ± 4.9	-7 ± 17		54.1 ± 1.6	-42 ± 5	
11	oxydiacetic	18.9 ± 0.5	4.3 ± 0.2	51.1 ± 0.5	-49 ± 2		63.0 ± 3.6	-22 ± 12	
12	L-malic	18.6 ± 0.4	5.3 ± 0.1	53.5 ± 0.9	-41 ± 3		57.0 ± 2.1	-40 ± 7	
13	citric	16.4 ± 0.4	3.6 ± 0.1	56.4 ± 1.7	-32 ± 6	-3.5 ± 0.2	58.9 ± 2.5	-34 ± 8	-1.9 ± 0.4

^a Data from ref 10. ^b Calculated at 298 K.

Table 4. Equilibrium Constants K_1 , Stability Constants β_1 , and Thermodynamic Parameters (ΔH_1° , ΔS_1° , and ΔV_1°) Associated with K_1 at 25 °C and $\mu = 1.00$ M

no.	RCOOH	$K_1^{298} b$	$\beta_1^{298} c/\text{M}^{-1}$	$\Delta H_1^\circ d/(\text{kJ mol}^{-1})$	$\Delta S_1^\circ e/(\text{J K}^{-1} \text{mol}^{-1})$	$\Delta V_1^\circ f/(\text{cm}^3 \text{mol}^{-1})$
1	formic	1.4 ± 0.1	(4.7 ± 0.3) × 10 ³	-9.7 ± 1.4	-29 ± 4	
2	acetic ^a	0.59 ± 0.02	(2.19 ± 0.09) × 10 ⁴	-5.0 ± 0.8	-21 ± 2	-6.4 ± 0.5
3	propionic ^a	0.45 ± 0.05	(2.10 ± 0.24) × 10 ⁴	-1.5 ± 0.9	2 ± 3	-7.2 ± 1.0
4	butyric	0.51 ± 0.02	(2.4 ± 0.1) × 10 ⁴	-14.6 ± 2.6	-55 ± 9	
5	glycolic ^a	1.54 ± 0.03	(6.4 ± 0.1) × 10 ³	-5.6 ± 1.0	-15 ± 3	-1.1 ± 0.4
6	DL-lactic	1.42 ± 0.03	(6.2 ± 0.1) × 10 ³	-6.6 ± 3.3	-18 ± 11	
7	2-methylactic	1.88 ± 0.06	(1.11 ± 0.04) × 10 ⁴	-8.1 ± 1.3	-21 ± 5	
8	methoxyacetic	1.60 ± 0.05	(4.02 ± 0.03) × 10 ³	-6.8 ± 6.5	-18 ± 21	
9	malonic	6.3 ± 0.2	(2.5 ± 0.1) × 10 ³	-7.5 ± 0.3	-10 ± 2	-2.2 ± 0.7
10	succinic	1.2 ± 0.2	(1.07 ± 0.18) × 10 ⁴	10 ± 7	36 ± 22	
11	oxydiacetic	4.4 ± 0.3	(2.9 ± 0.2) × 10 ³	-12 ± 3	-27 ± 10	
12	L-malic	3.5 ± 0.1	(4.5 ± 0.1) × 10 ³	-3.5 ± 3.0	-1 ± 10	
13	citric	4.6 ± 0.2	(2.9 ± 0.1) × 10 ³	-3.4 ± 4.2	2 ± 14	-1.6 ± 0.6

^a Data from ref 10. ^b Calculated as k_1/k_{-1} . ^c Calculated as K_1/K_{a1} . ^d Calculated as $\Delta H_1^\circ = \Delta H_1^\ddagger - \Delta H_{-1}^\ddagger$. ^e Calculated as $\Delta S_1^\circ = \Delta S_1^\ddagger - \Delta S_{-1}^\ddagger$. ^f Calculated as $\Delta V_1^\circ = \Delta V_1^\ddagger - \Delta V_{-1}^\ddagger$.

Table 5. Ionic Strength Dependencies of Rate Constants for the Reaction between $\text{Pd}(\text{H}_2\text{O})_4^{2+}$ and L-Malic Acid at 25 °C^a

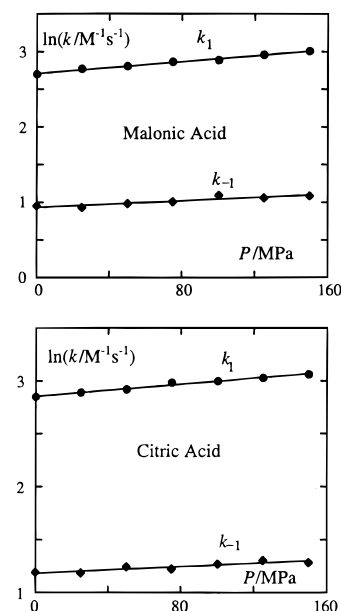
μ/M	$k_1/(\text{M}^{-1} \text{s}^{-1})$	$k_{-1}/(\text{M}^{-1} \text{s}^{-1})$
0.50	18.5 ± 0.3	4.8 ± 0.2
1.00	18.6 ± 0.4	5.3 ± 0.1
1.50	18.7 ± 0.6	5.9 ± 0.2
2.00	19.3 ± 0.7	6.8 ± 0.2

^a Rate constants were derived by use of the data in Supporting Information Table S14.

High-Pressure Kinetics. Volume profiles have been established earlier for the reactions of $\text{Pd}(\text{H}_2\text{O})_4^{2+}$ with acetic, propionic, and glycolic acids.¹⁰ In order to study how the partial molar volumes of the entering ligands influences the volumes of activation, variable-pressure data for malonic and citric acids were determined. Values of k_{obsd} were measured as a function of [carboxylic acid] at 25 °C and $[\text{H}^+] = 1.00$ M between 0.1 and 150 MPa. Values of k_1 and k_{-1} were calculated at different pressures by use of the data in Supporting Information Tables S11 and S12. Plots of $\ln k_1$ and $\ln k_{-1}$ vs pressure are shown in Figure 5. Volumes of activation were evaluated by fitting eq 9 to these data, with k_0 and ΔV^\ddagger as adjustable parameters,

$$\ln k = \ln k_0 - \Delta V^\ddagger P/RT \quad (9)$$

and with k_0 denoting the second-order rate constants (k_1 and k_{-1} , respectively) at zero pressure. No significant pressure dependence of the volumes of activation was observed. Volumes of activation, ΔV_1^\ddagger and ΔV_{-1}^\ddagger , and partial molar reaction volumes calculated as $\Delta V_1^\circ = \Delta V_1^\ddagger - \Delta V_{-1}^\ddagger$ are listed in Tables 3 and 4, respectively.

**Figure 5.** Pressure dependence of forward and reverse rate constants for reaction 1 at 25 °C according to eq 9.

Discussion

Equilibrium and Stability Constants. The equilibrium constants derived from the spectrophotometric equilibrium measurements are in good agreement with those evaluated from the kinetics, confirming that all reactions studied are described by eq 1; cf. Table 2. The variation of the equilibrium constants K_1 parallels the change of K_{a1} (cf. Tables 1 and 4). Although

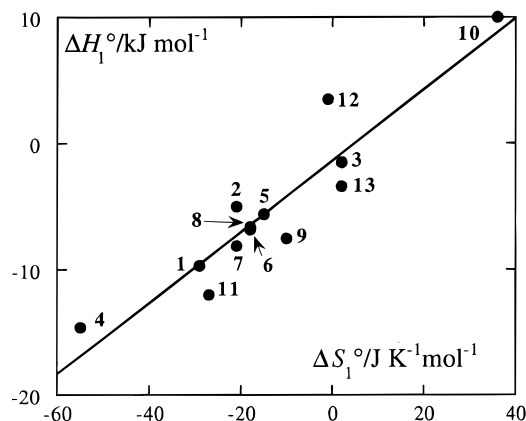


Figure 6. Compensation effect between ΔH_1° and ΔS_1° . Ligand numbers are indicated in Table 4.

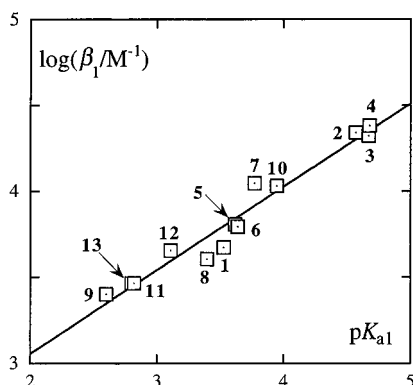


Figure 7. Linear free energy relationship between stability constants of palladium(II) carboxylate complexes and pK_{a1} values at 25 °C. Ligand numbers refer to those listed in Table 4.

the structural differences between the carboxylic acids used are large, the equilibrium constants K_1 vary only from 0.45 to 6.3. This is due to a compensation effect between ΔH_1° and ΔS_1° , as shown in Figure 6. As a result, the change in ΔG_1° for reaction 1 is quite small. The linear relation between ΔH_1° and ΔS_1° indicates that the bonds formed between palladium(II) and the carboxylates are of a similar type for all carboxylic acids studied.

Although reaction between $\text{Pd}(\text{H}_2\text{O})_4^{2+}$ and the carboxylate anions RCOO^- is negligible for $0.60 \leq [\text{H}^+] \leq 1.00$ M, the stability constants β_1 can be calculated from eq 10. Values are

$$\beta_1 = \frac{[\text{Pd}(\text{H}_2\text{O})_3\text{OOCR}^+]}{([\text{Pd}(\text{H}_2\text{O})_4^{2+}][\text{RCOO}^-])} = \frac{K_1}{K_{a1}} \quad (10)$$

given in Table 4. As expected, the stabilities of the monodentate complexes increase when the carboxylic acids become weaker. The influence of the substituents R on the affinity of the carboxylate ion for $\text{Pd}(\text{H}_2\text{O})_4^{2+}$ relative to H^+ is illustrated in Figure 7. There is a linear correlation between the stability constants for the carboxylate complexes and the first protolysis constants of the corresponding carboxylic acids, as described by eq 11, suggesting that the substituents R affect the stability

$$\log \beta_1 = (0.48 \pm 0.03)pK_{a1} + (2.2 \pm 0.1) \quad (11)$$

constants of palladium(II) carboxylate complexes in a way similar to their effect on the protolysis constants. Steric factors seem to have a negligible influence as evidenced from the fact that the bulky citric acid (**13**) and the long-chain oxydiacetic acid (**11**) do not deviate from the linear correlation between $\log \beta_1$ and pK_{a1} . Thus, the stability constants of the palla-

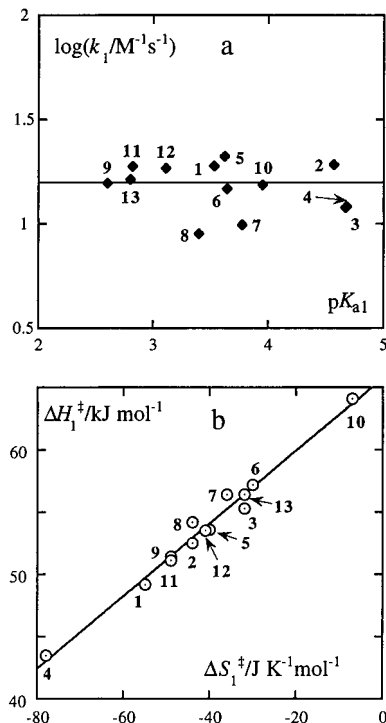


Figure 8. (a) Plot of $\log k_1$ as a function of pK_{a1} at 25 °C and 1.00 M ionic strength. (b) Isokinetic relationship between ΔH_1^\ddagger and ΔS_1^\ddagger for the forward reaction of eq 1. Ligand numbers are indicated in Table 3.

dium(II) carboxylate complexes are mainly determined by the electronic properties of the ligands. The relative magnitude of $\log \beta_1$ and pK_{a1} indicates that the carboxylate ions have an almost equal affinity for $\text{Pd}(\text{H}_2\text{O})_4^{2+}$ and H^+ , despite the higher positive charge of $\text{Pd}(\text{H}_2\text{O})_4^{2+}$. The slope of 0.48 of the line in Figure 7 indicates that the variation of the substituents R have a greater influence on $\Delta(\Delta G_a^\circ)$ than on $\Delta(\Delta G_f^\circ)$, where ΔG_a° and ΔG_f° denote the free energy changes for carboxylic acid protolysis and for complex formation between Pd(II) and carboxylate, respectively. This observation is in agreement with the hard-soft acid-base concept, carboxylate ion and proton being hard whereas Pd(II) is a soft acid. Accordingly, pK_{a1} values are expected to be more sensitive to the variation of the substituents R than $\log \beta_1$.

Rate Constants. The present results, together with those reported previously,¹⁰ allow us to examine in detail how the nature of the carboxylic acids influences their reactivities. The formation rate constants k_1 change only from 9.0 for methoxyacetic acid to $21.1 \text{ M}^{-1} \text{ s}^{-1}$ for glycolic acid at 298 K (Table 3), although the pK_{a1} values vary from 2.60 to 4.70. The pK_{a1} value can be used as a measure of the electron-donating or -withdrawing capacity of a specific carboxylic acid. A plot of $\log k_1$ versus pK_{a1} is shown in Figure 8a. It is obvious that the formation rate constants are virtually independent of pK_{a1} . Steric factors do not seem to have any influence on the reactivities of the entering carboxylic acids. Thus, the rate constants k_1 remain essentially unchanged from formic acid to the bulky citric acid. These observations are in contrast to our findings for the reactions between $\text{Pd}(\text{H}_2\text{O})_4^{2+}$ and thioethers,⁹ where electronic and steric properties of the entering nucleophiles are sensitively reflected in and correlated with their reactivities, and also to the usual strong entering ligand dependence observed for substitution reactions at palladium(II).^{23–26}

However, the enthalpies and entropies of activation for the forward process of eq 1 vary significantly (Table 3). A plot of

(23) Helm, L.; Elding, L. I.; Merbach, A. E. *Helv. Chim. Acta* **1984**, *67*, 1453–1460.

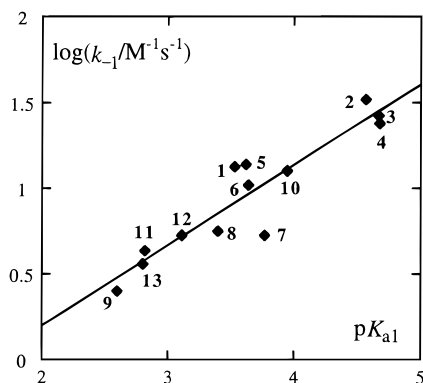


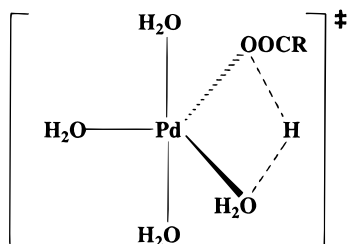
Figure 9. Linear correlation between $\log k_{-1}$ and pK_{a1} at 25 °C. Ligand numbers are listed in Table 3.

activation parameters for this process (Figure 8b) shows an excellent isokinetic relationship between ΔH_1^\ddagger and ΔS_1^\ddagger , again suggesting that all of the carboxylic acids react via the same mechanism.¹ Furthermore, the isokinetic temperature is 292 ± 13 K, i.e., very close to 25 °C. As a result, the differences in ΔG_1^\ddagger at 25 °C for the carboxylic acids studied are quite small, which explains why the formation rate constants are very similar at room temperature.

There is a large variation of the rate constants k_{-1} with the nature of the carboxylic acids (Table 3). Since the k_1 values remain approximately constant and $K_1 = k_1/k_{-1}$, the values of K_1 are governed by k_{-1} at room temperature. Figure 9 displays the correlation between $\log k_{-1}$ and pK_{a1} as described by eq 12, indicating that the weaker the carboxylic acid, the larger

$$\log k_{-1} = (0.47 \pm 0.06)pK_{a1} - (0.7 \pm 0.2) \quad (12)$$

the value of k_{-1} . On the other hand, eq 11 shows that a weaker carboxylic acid such as acetic acid is prone to form a stronger complex. These facts, together with the direct attack of an oxonium ion on $\text{Pd}(\text{H}_2\text{O})_3\text{OOCR}^+$ in the reverse reaction of eq 1, as indicated by the experimental rate law and the ionic strength dependence of k_{-1} , can be interpreted in terms of a proton-assisted reaction. A transition state stabilized by hydrogen bonding, shown as follows,



and as proposed previously^{10,27} can account for the reactivity trend predicted by eq 12. The conjugate carboxylate of a weaker carboxylic acid is a better electron donor and can form a stronger hydrogen bond which in turn stabilizes the transition state and decreases ΔH_{-1}^\ddagger . Since the overall change of ΔG_{-1}^\ddagger is only ca. 7 kJ mol⁻¹ at 25 °C (calculated as $\Delta G_{-1}^\ddagger = \Delta H_{-1}^\ddagger -$

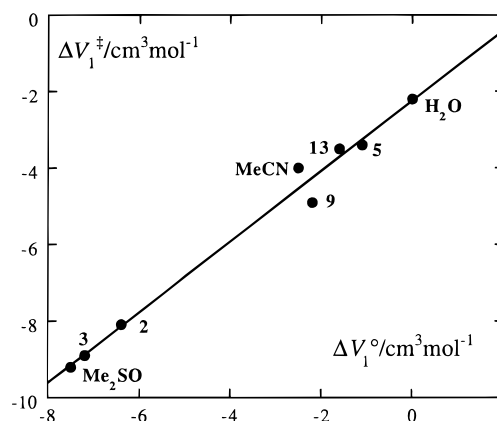


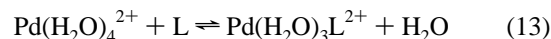
Figure 10. Linear correlation between ΔV_1^\ddagger and ΔV_1° at 25 °C for $\text{Pd}(\text{H}_2\text{O})_4^{2+}$ reactions. Ligand numbers refer to those listed in Table 1.

$T\Delta S_{-1}^\ddagger$), this change might well be due to fluctuations in hydrogen bond strength.

Another conclusion that can be drawn from the fact that a stronger complex exhibits a higher k_{-1} is that bond-breaking cannot make a substantial contribution to the activation process in these systems. If this was the case, the observed reactivity trend of k_{-1} would have been opposite to that described by eq 12. Thus, the activation process for substitution at $\text{Pd}(\text{H}_2\text{O})_4^{2+}$ is dominated by bond-making, which is also indicated by numerous other experimental observations.^{9,10,23–26}

Volumes of Activation and Reaction Mechanism. The values of ΔV_1^\ddagger vary significantly with the nature of the entering carboxylic acids, whereas those of ΔV_{-1}^\ddagger are almost equal within experimental errors; cf. Table 3. These findings indicate that bond-making with the entering ligands is important in the activation process and that the leaving group is still tightly bound to the metal center in the transition state.^{10,25} The facts that ΔH_1^\ddagger and ΔS_1^\ddagger vary considerably with the nature of the carboxylic acids and that ΔH_{-1}^\ddagger and ΔS_{-1}^\ddagger remain essentially constant are also consistent with carboxylic acid participation in the transition state.

A plot of ΔV_1^\ddagger as a function of ΔV_1° for reaction 1 is shown in Figure 10. Also included are data for reaction 13 with L =



H_2O ,²³ Me_2SO ,²⁴ and MeCN .²⁵ It is noteworthy that the data for reactions 1 and 13 fall upon a common straight line defined by eq 14, although they differ by the participation of one proton. This implies that the transition states for reactions 1 and 13 are similar.

$$\Delta V_1^\ddagger = (0.92 \pm 0.04) \Delta V_1^\circ - (2.2 \pm 0.2) \text{ cm}^3 \text{ mol}^{-1} \quad (14)$$

Linear relationships between ΔV^\ddagger and ΔV° were first observed by Swaddle^{28,29} and have since been reported and used for deduction of mechanisms. For the hydrolysis of $\text{Co}(\text{NH}_3)_5\text{X}^{n+}$, where X = SO_4^{2-} , Cl^- , Br^- , NO_3^- , and H_2O , the slope of the ΔV^\ddagger vs ΔV° plot is unity, indicating that bond-breaking dominates the activation process.²⁸ On the other hand, data for hydrolysis of a series of $\text{Cr}(\text{NH}_3)_5\text{X}^{n+}$ complexes give a slope of 0.59,²⁹ interpreted as indicating 50% bond-stretching in the transition state; i.e., charge separation and concomitant changes in electrostriction are assumed to be 50% complete in the

(24) Ducommun, Y.; Merbach, A. E.; Hellquist, B.; Elding, L. I. *Inorg. Chem.* **1987**, *26*, 1759–1963.

(25) Hellquist, B.; Elding, L. I.; Ducommun, Y. *Inorg. Chem.* **1988**, *27*, 3620–3623.

(26) Elmroth, S.; Bugarcic, Z.; Elding, L. I. *Inorg. Chem.* **1992**, *31*, 3551–3554.

(27) A similar hydrogen-bond-stabilized transition state was recently proposed for fluoride exchange at uranyl(2+) complexes: Szabo, Z.; Glaser, J.; Grenthe, I. *Inorg. Chem.* **1996**, *35*, 2036–2044.

(28) Jones, W. E.; Carey, L. R.; Swaddle, T. W. *Can. J. Chem.* **1972**, *50*, 2739–2746.

(29) Guastalla, G.; Swaddle, T. W. *Can. J. Chem.* **1973**, *51*, 821–827.

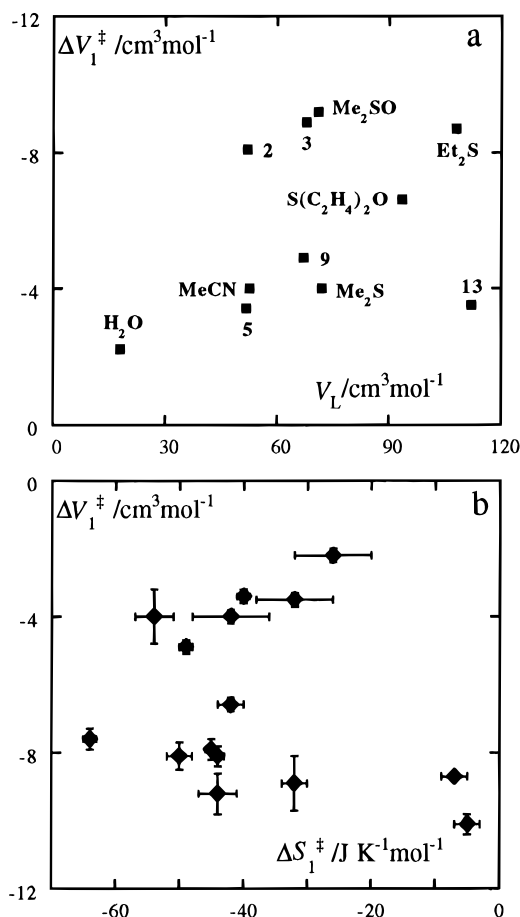


Figure 11. (a) Plot of ΔV_1^\ddagger vs the partial molar volume (V_L) of the entering ligands. (b) ΔV_1^\ddagger as a function of ΔS_1^\ddagger for $\text{Pd}(\text{H}_2\text{O})_4^{2+}$ reactions. Ligand numbers refer to those listed in Table 1.

transition state,²⁹ a proposal later substantiated by a study of individual partial molar volumes.³⁰ Similar arguments have been used by Palmer and Kelm³¹ for the hydrolysis of $\text{Pd}(\text{teden})\text{-X}^+$ and by van Eldik and co-workers³² for anation reactions of $\text{Pd}(\text{R}_5\text{dien})\text{H}_2\text{O}^{2+}$, where $\text{teden} = N'-[2-(\text{diethylamino})\text{ethyl}]-N,N$ -diethylethane-1,2-diamine and $\text{dien} = \text{diethylenetriamine}$. If we adopt this reasoning, the slope of 0.92 for the linear plot between ΔV_1^\ddagger and ΔV_1° for the present reaction systems should indicate that the formation of the transition state is largely dominated by bond-making between $\text{Pd}(\text{H}_2\text{O})_4^{2+}$ and the entering ligands. In other words, the mechanisms for reactions 1 and 13 are strongly I_a .

Relations between ΔV_1^\ddagger and V_L and ΔS_1^\ddagger . Anation reactions of $\text{Pd}(\text{R}_5\text{dien})\text{H}_2\text{O}^{2+}$ ($\text{R} = \text{Me}$ and Et) with thiourea and derivatives as well as water exchange have been concluded to proceed via a similar mode of activation,^{33,34} and linear correlations between ΔV^\ddagger and the partial molar volumes (V_L) of the entering ligands have been reported. It has been argued that a larger V_L makes a bigger overlap of the van der Waals radii, which in turn should give rise to a more negative activation volume.^{33,34} An examination of this relation for the present systems can be based on a much more complete experimental material. It is obvious from the plot in Figure 11a not only

Table 6. Entropies and Volumes of Activation at 25 °C for Complex Formation Reactions between $\text{Pd}(\text{H}_2\text{O})_4^{2+}$ and Various Entering Ligands

entering ligand	ΔS_1^\ddagger / ($\text{J K}^{-1} \text{mol}^{-1}$)	ΔV_1^\ddagger / ($\text{cm}^3 \text{mol}^{-1}$)	ref
H_2O	-26 ± 6	-2.2 ± 0.2	23
Me_2SO	-44 ± 3	-9.2 ± 0.6	24
MeCN	-54 ± 3	-4.0 ± 0.8	25
Me_2S	-42 ± 6	-4.0 ± 0.2	26
Et_2S	-7 ± 2	-8.7 ± 0.1	26
$\text{S}(\text{C}_2\text{H}_4)_2\text{S}$	-5 ± 2	-10.1 ± 0.3	26
$\text{S}(\text{C}_2\text{H}_4)_2\text{O}$	-42 ± 2	-6.6 ± 0.2	26
$\text{S}(\text{CH}_2\text{CH}_2\text{COOH})_2$	-64 ± 1	-7.6 ± 0.3	9
$\text{EtSCH}_2\text{COOH}$	-45 ± 1	-7.9 ± 0.5	9
$\text{S}(\text{CH}_2\text{COOH})_2$	-50 ± 2	-8.1 ± 0.4	9
CH_3COOH (2)	-44 ± 1	-8.1 ± 0.3	10
$\text{CH}_3\text{CH}_2\text{COOH}$ (3)	-32 ± 2	-8.9 ± 0.8	10
HOCH_2COOH (5)	-40 ± 1	-3.4 ± 0.2	10
$\text{HOOCCH}_2\text{COOH}$ (9)	-49 ± 1	-4.9 ± 0.2	this work
$\text{HOOC}(\text{OH})(\text{CH}_2\text{COOH})_2$ (13)	-32 ± 6	-3.5 ± 0.2	this work

that the linear correlation proposed does not exist in our case, but also that the trend that a larger V_L is accompanied by a more negative ΔV_1^\ddagger is very weak. As a matter of fact, there seems to be no theoretical basis for such linear correlations for associative substitutions at square-planar metal centers.

According to a recent model for leaving group effects on volumes of activation for dissociative processes,³⁵ the volume of the leaving ligand is subdivided into one part (V_a) situated inside the coordination sphere and another (V_b) outside the volume defined by the nonreacting ligands. By analogy, subdividing the volume of the entering ligand in an associative process into two parts in the transition state, it can be readily shown that the volume of activation should be independent of V_b and a linear function of V_a , which for polyatomic ligands with a constant donor atom should depend on the ligand cone angles. So far, there is not sufficient steric data available for the ligands in Table 6. However, data for thioethers⁹ might be consistent with such model.

Entropies and volumes of activation are generally believed to stem from the same origin. Indeed, Laidler,³⁶ Twigg,³⁷ and Lawrance *et al.*³⁸ have reported linear correlations between ΔV^\ddagger and ΔS^\ddagger for a number of systems. Data of ΔS_1^\ddagger and ΔV_1^\ddagger for $\text{Pd}(\text{H}_2\text{O})_4^{2+}$ complex formation reactions are collected in Table 6. Here again, there is no linear relation between ΔV_1^\ddagger and ΔS_1^\ddagger , although a single metal center and the same activation mode are involved, as illustrated by Figure 11b.

Conclusion

Comprehensive rate and equilibrium data including variable-temperature and -pressure data have been determined for reactions between tetraaquapalladium(II) and a large series of carboxylic acids. Together with previous data for reactions between the substrate complex and other nucleophiles, these results enable the construction of various linear free energy relationships. (i) The equilibrium constants K_1 vary only slightly with the nature of the carboxylic acids, although the structural differences between these acids are large. This is due to a compensation effect between ΔH_1° and ΔS_1° as shown by a linear relation between these parameters. (ii) A linear correlation between $\log \beta_1$ for the 1:1 monocarboxylato complexes formed and $\text{p}K_{a1}$ for the corresponding carboxylic acids shows that the stability constants are determined by electronic effects, whereas

(30) Palmer, D. A.; Kelm, H. *Inorg. Chem.* **1977**, *16*, 3139–3143.

(31) Palmer, D. A.; Kelm, H. *Aust. J. Chem.* **1979**, *32*, 1415–1424.

(32) Pienaar, J. J.; Kotowski, M.; van Eldik, R. *Inorg. Chem.* **1989**, *28*, 373–375.

(33) Hellquist, B.; Elding, L. I.; Merbach, A. E.; Ducommun, Y.; Helm, L.; van Eldik, R. *High Pressure Res.* **1990**, *5*, 672–674.

(34) Berger, J.; Kotowski, M.; van Eldik, R.; Frey, U.; Helm, L.; Merbach, A. E. *Inorg. Chem.* **1989**, *28*, 3759–3765.

(35) Jordan, R. B. *Inorg. Chem.* **1996**, *35*, 3725–3726.

(36) Laidler, K. J. *Chemical Kinetics*, 3rd ed.; Harper Collins: New York, 1987; pp 208–210.

(37) Twigg, M. V. *Inorg. Chim. Acta* **1977**, *24*, L84–L86.

(38) Lawrance, G. A.; Suvachittanon, S. *Inorg. Chim. Acta* **1979**, *32*, L13–L15.

the steric properties of the carboxylate ligands seem to have a negligible influence. (iii) Formation rate constants k_1 at 25 °C remain essentially constant, independent of electronic and structural differences between the entering carboxylic acids. This is due to an isokinetic relationship between ΔH_1^\ddagger and ΔS_1^\ddagger , with an isokinetic temperature of 292 ± 13 K, i.e., close to room temperature. (iv) Rate constants k_{-1} vary significantly with the nature of the carboxylic acids, and $\log k_{-1}$ varies linearly with $\text{p}K_{\text{a}1}$; i.e., the weaker the carboxylic acid, the larger the value of k_{-1} . (v) This fact, together with the experimental rate law and the ionic strength dependence of k_{-1} indicates a proton-assisted reaction, with a transition state stabilized by hydrogen bonding. (vi) ΔH_1^\ddagger , ΔS_1^\ddagger , and ΔV_1^\ddagger vary considerably with the nature of the carboxylic acids, whereas ΔH_{-1}^\ddagger , ΔS_{-1}^\ddagger , and ΔV_{-1}^\ddagger remain virtually constant, indicating that bond-making with the entering ligands is important in the activation process and that the leaving group is still tightly bound to the metal center in the transition state. (vii) The slope of 0.92 for the linear correlation between ΔV_1^\ddagger and ΔV_1° also indicates that formation of the transition state is largely dominated by bond-making. The mechanism can be characterized as strongly I_{a} . (viii) For substitution at $\text{Pd}(\text{H}_2\text{O})_4^{2+}$, there are no linear correlations between ΔV_1^\ddagger and the partial molar volumes of the ligands, V_{L} , as claimed for related reactions in previous literature, or between ΔV_1^\ddagger and ΔS_1^\ddagger .

Acknowledgment. Financial support from the Swedish Natural Science Research Council and a grant from the K. and A. Wallenberg Foundation for the high-pressure equipment are gratefully acknowledged. Dr. Z. Burgarcic is thanked for some preliminary studies of the oxydiacetic acid reaction.

Registry No. (Author Supplied): $\text{Pd}(\text{H}_2\text{O})_4^{2+}$, 22573-07-5; formic acid, 64-18-6; acetic acid, 64-19-7; propionic acid, 79-09-4; butyric acid, 107-92-6; glycolic acid, 79-14-1; DL-lactic acid, 50-21-5; 2-methylactic acid, 594-61-6; methoxyacetic acid, 625-45-6; malonic acid, 141-82-2; succinic acid, 110-15-6; oxydiacetic acid, 110-99-6; L-malic acid, 97-67-6; citric acid, 77-92-9.

Supporting Information Available: Observed pseudo-first-order rate constants as functions of acidity, carboxylic acid concentration, and temperature (Tables S1–S10) and as a function of pressure (Tables S11 and S12), equilibrium constants and molar absorption coefficients for some carboxylic acids (Table S13), ionic strength dependence of rate constants for the reaction of L-malic acid (Table S14), absorbance as a function of $[\text{RCOOH}]$ at different acidities (Figure S1), and k_{obsd} as a function of formic, lactic, 2-methylactic, and oxydiacetic acid concentrations for various $[\text{H}^+]$ according eq 7 (Figure S2) (11 pages). Ordering information is given on any current masthead page.

IC9613523